

Experimental study of chemical oxygen demand removal by electrochemical oxidation treatment of petroleum refinery wastewater by using response surface methodology

Maad A. Hussein^{a,*}, Hassan A. Shamkhi^b, Zahraa N. Abd^b, Fatima H. Abbas^b

^aDepartment of Environmental Science, College of Energy and Environmental Sciences, Al-Karkh University of Science, Baghdad 10081, Iraq, email: altaaimaad@yahoo.com/maad@kus.edu.iq (M.A. Hussein)

^bDepartment of Chemical and Petroleum Industries Engineering, Al-Mustaqbal University College, Babylon 51001, Iraq, emails: hassan.ali@mustaqbal-college.edu.iq (H.A. Shamkhi), zahraa.nadhun@mustaqbal-college.edu.iq (Z.N. Abd), fatima.hamid.abbas@uomus.edu.iq (F.H. Abbas)

Received 22 September 2022; Accepted 4 December 2023

ABSTRACT

The current study uses a batch electro-chemical reactor with porous graphite as an anode and a stainless steel as a cathode for wastewater treatment taken from the Al-Najaf petroleum refinery plant, Iraq. On removal efficiency regarding chemical oxygen demand (COD), the impacts of operating conditions like pH (2–10), current density (5–25 mA/cm²), time (30–70 min), and NaCl addition (0–4 g/L) were explored. The findings demonstrated that both NaCl and pH have an important effect on the removal efficiency of the COD, indicating the fact that the system is regulated through the reaction situations in the bulk of the solution rather than electrooxidation regarding the chloride ions on an electrode surface. For maximizing COD removal, response surface methodology was integrated with a Box–Behnken design in parametric optimization. COD's removal percentage was determined to be 99.6% under optimized operating parameters of a current density = 25 A/cm², initial pH: 2, time = 65 min, and NaCl concentration = 3.39 g/L, with 9.85 kWh/kg-COD energy consumption, which is lower when compared to similar works.

Keywords: Petroleum refinery; Wastewater; Porous graphite; Indirect oxidation; Response surface methodology; Chemical oxygen demand removal

1. Introduction

Crude oil is converted into its main components using thermal, physical and chemical separation processes, and after that such fractions are then processed by a set of steps of separation and conversion in order to produce the final products like gasoline, liquefied petroleum gas, kerosene, diesel-fuel, lubricating oil, and other products. In refining processes, fresh water is used in several stages such as, mostly for hydrotreating, distillation, cooling and desalting systems [1]. Approximately 80%–90% of water that is utilized in the refinery processes are converted to wastewater.

Aljuboury et al. [2] had found that the amount (as volume) regarding the effluents created during the processing of the crude oil has been 0.40–0.60 times as much as the quantity (i.e., volume) of processed crude-oil.

The manufacturing method, kind of oil, and process configuration all influence the composition of created wastewaters. Chemical oxygen demand (COD) concentrations of almost 350–650 mg/L, benzene concentrations of 1–100 mg/L, phenol concentrations of 10–250 mg/L, heavy metal concentrations of lead (0.20–10 mg/L), chromium (0.10–100 mg/L), besides other pollutants are found in the polluted wastewater created via refineries [3]. Because of

* Corresponding author.

high presence of polycyclic aromatic compounds, which have particularly harmful impacts on environment and can exist for long periods in the environment, direct disposal of such wastewaters can cause significant pollution problems for the environment. As a result, such effluents must be treated before being discharged [4].

The most prevalent approach for treating wastewater created by refinery plants is to use physicochemical and mechanical approaches, followed by the biological treatments in a unit of integrated activated-sludge treatment. Wet oxidation [5], photo-catalytic oxidation [6], catalytic vacuum distillation [7], photodegradation [8], Fenton-oxidation [9], coagulation–flocculation [10], membrane [11–13], adsorption [14], chemical precipitation [15], and membrane bioreactor [16] are some of the other treatment approaches investigated by the researchers. Generally, the key concepts regarding the majority of such approaches are the low-efficiency conversion of the pollutants from a medium to a different one.

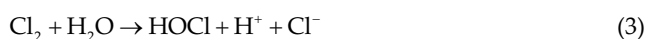
Electrochemical oxidation (EO) treatment was utilized for treating a variety of the industrial wastewater, which include those from pulp and paper plants, tanneries, distilleries, and the textile sector. Also, the literature mentions EO destruction regarding the wastewaters that contain the phenolic compounds like the poly-aromatic organic complexes, dyes, arsenic, and sulfidic wasted caustic [17]. The EO approach is a safe and effective way to mineralize organic contaminants in water. Since the principal reagent utilized is the electron, this approach has gained a lot of interest due to its safety, versatility, energy efficiency, selectivity, automation ability, cost effectiveness, and environmental compatibility. EO, unlike photochemical or chemical oxidation, does not require using or storing hazardous substances, and it is easier to scale up [18].

Contaminants could be degraded through indirect or direct oxidation [19] mechanisms throughout EO process as illustrated. Organic pollutants are adsorbed on anode's surface and subsequently demolished *via* direct electron transfer in a direct route. The indirect technique involves electrochemically producing strong oxidants like the hydrogen peroxide, ozone, and hypochlorite/chlorine, reacting with organic pollutants in bulk solution [20]. Because dyes are commonly present in wastewaters, chloride is especially appealing for the utilization in the indirect oxidation [21]. Researchers have thoroughly researched the active chlorine role in breakdown of the dyes as well as other organic compounds in the literature. Due to improvements in current efficiency and oxidation kinetics, along with a decrease in cell potential, adding chloride ions to the effluent will reduce energy consumption [22].

The anodic reactions are as follows:



The bulk reactions are as follows:



The cathodic reactions are as follows:



In the case where an appropriate chloride ions amount is present in wastewater, Cl_2 is produced anodically as in Eq. (1) and forming OCl^- as in Eq. (5), respectively which may be utilized for the destruction and elimination of the oxidizable organic pollutants.

Complex interaction of numerous parameters which can be tuned to produce an affordable and successful process is identified *via* the performance of EO methods in the removing of pollutants. Electrode potential; regime of mass transport; current density; pH; current distribution; electrode materials; conductivity; design of the cell; and types of contaminants are the primary parameters that impact the efficacy of an EO process [23]. As a result, the EO process is seen as a complex process that necessitates statistically designed experiments in order to decrease the number of experimentations and improve combination of input components. Statistical design reduces the variability of the process and the time needed for trial-and-error experimentations [24]. Response surface methodology (RSM) has been considered as a substantial topic in designing the statistical experiments. It has been successfully used in chlorine disinfection [25], adsorption [26], Fenton-related processes [27], and electrocoagulation [28] for wastewater treatment. It is made up of a combination of statistical and mathematical methods which may be utilized in order to analyze and model various problems where multiple characteristics impact a desired result. RSM's goal is to assess relative influence of various influencing parameters and then optimize this response to attain the ideal operating conditions [29].

Despite the fact that EO techniques have a wide-ranging of applications for treating many categories of wastewaters, literature on their usage for treating wastewater that is generated by petroleum refineries is limited. In previous studies, the electrode material was found to be a critical component in determining efficiency of EO process for treating petroleum refinery effluents since the electrode material might alter the oxidation and anodic reactions mechanisms. For instance, Treviño-Reséndez et al. [30] examined the treatment of wastewaters arising from petroleum refinery by utilizing indirect and direct EO *via* 2 types of the anode, which are: ruthenium mixed metal oxide (Ru-MMO) and boron-doped diamond (BDD) [31]. In their study, Martínez-Huitle and Brillas [32] employed BDD, whereas, Ajab et al. [33] utilized Ru-MMO electrodes for treating effluents in an oil refinery. Recently, Ghanim and Hamza [34] looked into using a PbO_2 anode to treat wastewater from a petroleum refinery. According to the kind of oxidation and the contaminants' composition, all of the above electrodes offer numerous benefits and drawbacks.

The current study represents process of the direct anodic oxidation for treatments of wastewater of petroleum refinery that is generated at the Al-Najaf refinery facility, which uses the design of experiments as an optimization approach and uses porous graphite with a high level of the specific surface area as anode solid. Process parameters have been optimized with the use of the Box–Behnken design (BBD). A quadratic model was established based on experiments using RSM's design matrix for input elements like the current density, initial pH, time and NaCl content. The ideal parametric values for COD elimination were determined using such quadratic model. Porous graphite has been selected as an anode because of its have a big specific area, availability, and inexpensive costs, besides its role as an anode material in indirect anodic oxidations [35]. Also, because the study is applied to real wastewater, it is possible and easy to scale up the system, and this means that there is great potential for the study to be applied industrially. Graphite has low over-potential values for the reaction of the oxygen evolution. Porous graphite electrodes are widely used to decompose the organic matter in the NaCl's presence due to their low process. Porous graphite has a wide surface area, a characteristic which can enhance the organic pollutants elimination rate via adsorbing and electro-chemical oxidations. None-the-less rather short graphite electrode life as a result to the corrosion of the surface is a disadvantage, particularly in the case where electro-oxidation takes place at high densities of the current.

2. Experimental work

The Al-Najaf petroleum refinery plant delivered samples of refinery effluent. The sample (40 L) has been taken from feeding tank to unit of biological treatment and kept inside covered containers at a temperature of 4°C till it was used. Table 1 summarizes the sample's characteristics. Aside from the characteristics of the effluent that has been taken from settling tank regarding final biological treatment stage which were evaluated *via* the administration of the petroleum refinery plant with an acceptable limit, the table included a comparison of the characteristics of the effluent that has been obtained from settling tank of final biological treatment stage. Raw water conductivity has been 1.92 mS/cm, and that value has been considered low and it causes cell potential to rise. To boost the conductivity of

the solution, a supporting electrolyte must be added. As a supporting electrolyte, sodium sulfate (Na_2SO_4) was used at a 0.05 M concentration, which results in final conductivity of 12.90 mS/cm, and that value has been considered within the needed range for obtaining low cell potential [36].

Anodic oxidation treatment studies were carried out in circular jacketed Perspex glass lab-scale batch electro-chemical cell with a Perspex cover. It has an inside diameter of 10 cm, a thickness of 0.5 cm, and a length of 20 cm, as well as a capacity of active electrolyte of 1 L. The cover has external dimensions of 13 cm external diameter and 1cm thickness, with two slits for electrode fixation and holes for the insertion of conductivity and pH meters probes, in addition to sample taking out. For electro-chemical reactor, stainless steel plate cathode (18 cm × 5 cm × 0.4 cm) and porous graphite anode (18 cm × 5 cm × 0.5 cm) were utilized in a parallel plate configuration. The anode and cathode distances were set to 2 cm. Throughout each experiment, digital power-supply of the direct current (0V–30V, 0A–5A) (Type 9 UNI-T, UTP3315PF) has been employed for providing constant current. In every run, 1.0 L of solution has been stirred with a magnetic stirrer at 500 rpm so that to produce proper conditions of mixing, after that requisite amount of supporting electrolyte and NaCl (whenever required) have been added, and mixing has been maintained at an identical speed of rotation throughout experiments. All of those experiments have been conducted in a water bath at a constant temperature of 28°C ± 2°C (Memmert, WNB-22, Germany).

The diagram related to electrochemical oxidation experimental setup has been depicted in Fig. 1, together with necessary data. pH value of the electrolyte has been monitored with digital-meter of the pH (HANNA Instruments Inc., PH-211, RI, USA) and acidity of electrolyte has been adjusted with NaOH/HCl for best experimental conditions. The materials used in the study like NaCl, Na_2SO_4 , NaOH and HCl are purchased from commercial suppliers, specifically from Thomas Baker (Mumbai, India).

The total organic compound concentration in effluent has been given in terms of (COD). In COD thermo-reactor (RD-125, Lovibond, Germany), the number of COD in effluents of the petroleum refinery has been determined through taking a (2 mL) sample that has been digested with $\text{K}_2\text{Cr}_2\text{O}_7$ as oxidizing agent for a period of 120 min at a temperature of 150°C. After cooling the digested sample

Table 1
Effluent properties at Al-Najaf petroleum refinery plant

Tests	Sample of the feed tank	Settling tank*	Acceptable limit*
Chemical oxygen demand (mg/L)	590–580	65	100
Total dissolved solids	920	1,700	–
pH	6.40	7.50	(6–9.5)
Cond. (mS/cm)	1.88	–	–
Cl (mg/L)	530	121	100
SO_4 (mg/L)	14.2	420	400
Turbidity	30.65	7.34	40.7
Phenol (mg/L)	0.165	(0.010–0.050)	0.060

*Presented by the administration of Al-Najaf petroleum refinery plant.

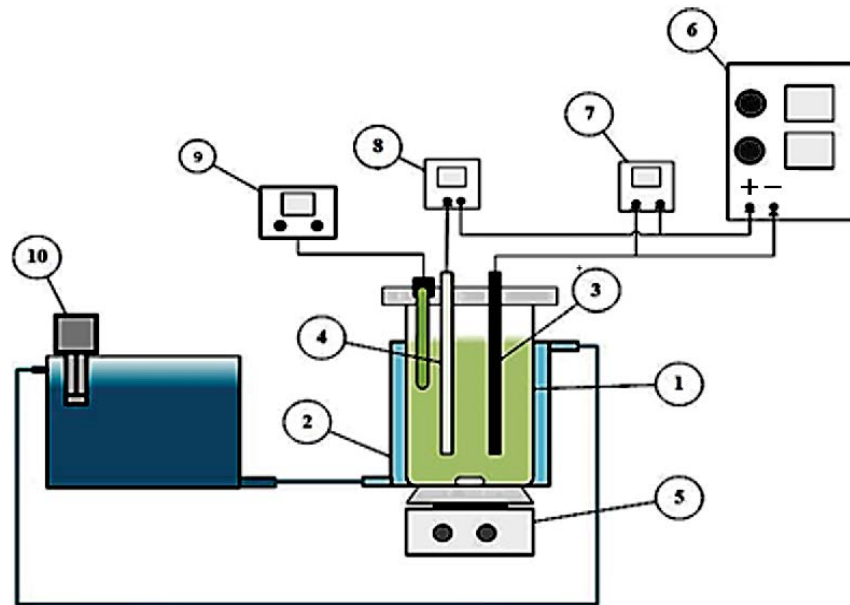


Fig. 1. Representation of experimental set-up: (1) body cell, (2) jacket, (3) porous graphite anode, (4) cathode, (5) magnetic stirrer, (6) power supply, (7) ammeter, (8) voltmeter, (9) pH-meter, (10) circulator of the water-bath.

to room temperature, it was examined in a spectrophotometer (MD200, Lovibond, Germany). Approach 8047, which has been assigned by Hach Co./Hach Lange GmbH, US, was used for the measurement of the phenol. The concentrations of COD and phenol have been measured for 3 times, and mean values are used in the present study.

2.1. Anode

As anode, porous graphite was employed. Scanning electron microscopy (SEM) using field emission scanning electron microscopy was used to analyze the topography of graphite surfaces. Graphite's total surface area has been measured with the use of Brunauer–Emmett–Teller (BET) technique and a device (BET Tavana, Iran) equipped with MicroActive for TriStar II Plus 2.03 software depending on Micrometrics.

The COD removal efficiency has been assessed according to Eq. (1) [37]:

$$RE\% = \frac{COD_i - COD_f}{COD_i} \times 100 \quad (9)$$

where RE% represents the removal percentage, COD_i signifies the initial COD (mg/L), and COD_f signifies final COD (mg/L).

In any anodic oxidation, the energy consumption (EC) denotes total of the energy that is spent during the procedure for a kilogram of the COD that must be digested. Eq. (2) can be used to obtain EC in (kWh/kg) [38]:

$$EC = \frac{E \cdot I \cdot t \times 1000}{(COD_i - COD_f)V} \times 100 \quad (10)$$

where EC denotes the consumption of the energy (kWh/kg-COD), I signifies current (A), E denotes applied cell voltage (Volt), COD_i and COD_f signifies final and initial COD (mg/L), t denotes time of electrolysis (h), and V denotes effluent volume (L).

2.2. Design of experimentations

RSM [39] could be used for determining the relation between process response and its variables by combining statistical and mathematical data. The three level, four factor Box–Behnken experimental design has been used in the present work for verifying and checking components that impact COD removal. The effectiveness of the COD removal has been used as response, whereas time (X_1), initial pH (X_2), NaCl concentration (X_3), and current density (X_4) were used as process variables. 0 (central or middle point), -1 (low level), and 1 (high level) were used to code the scales of process variables [40]. Table 2 shows parameters of the process and their respective levels. Box–Behnken creates and enhances designs that are required in order to obtain appropriate quadratic model with required statistical features while only using portion of runs that are needed for three-level factorial. Eq. (3) could be used for calculating the number of the runs (N) that are required in order to complete a Box–Behnken design [41]:

$$N = 2k(k-1) + cp \quad (11)$$

where k represents number of the variables of the process and c_p represent central point's reiterated number. A total of 27 runs have been conducted in the current study in order to assess effects of process variables upon the efficiency of COD removal. BBD that has been recommended for this work is depicted in Table 3.

According to BBD, a second-order polynomial-model could be used, with the next Eq. (4) denoting how the interaction terms fit with experimental data:

$$Y = a_0 + \sum a_i x_i + \sum a_{ii} x_i^2 + \sum a_{ij} x_i x_j \tag{12}$$

where Y denotes the response (RE), i & j represent pattern index numbers, a_0 represents intercept term, x_1, x_2, \dots, x_k

represent process variables in the coded forms. a_i represents first-order (linear) key effect, a_{ii} represents second-order main effect and a_{ij} represents interaction effect. Variance analysis has been carried out and after that, coefficient of regression (R^2) has been calculated for the purpose of confirming model fit goodness.

3. Results and discussions

3.1. Anode characterization

The porous graphite anode’s X-ray diffraction data are revealed in Fig. 2. It has the same reference code as the standard graphite structure (96-901-2231) (blue) [42]. The study of the structure of the graphite reveals sharp diffraction peak at $2\theta = 26.6255^\circ$, with d -spacing of 3.34802 Å for C(002). Fig. 3 illustrates a SEM image of the porous graphite anode with magnification power (7500). The graphite was discovered to have a high porosity, with big pores that have been developed between the inter-connected structures, as opposed to the conventional rigid graphite, which has a smooth nonporous structure. Porous graphite’s BET surface area was discovered equal to $22.7509 \pm 0.5307 \text{ m}^2/\text{g}$,

Table 2
Level of the process variables for the treatments of the refinery wastewater

Parameters of the process	Range in the design of Box–Behnken		
	Low [-1]	Middle [0]	High [+1]
X_1 - Time (min)	30	50	70
X_2 - pH	2	6	10
X_3 - NaCl (g/L)	0	2	4
X_4 - Current density (mA/cm ²)	5	15	25

Table 3
Experimental results of the Box–Behnken design for chemical oxygen demand removal

Run order	Block	pH	Current density (mA/cm ²)	NaCl (g/L)	Time (min)	RE%		E (V)	EC (kWh/kg-COD)
						Actual	Predict		
1	1	2	15	2	30	73	72.67	5.35	2.78
2	1	2	15	2	70	90	89.50	4.88	3.02
3	1	10	15	2	30	60	59.50	5.15	4.12
4	1	10	15	2	70	81	79.33	4	0.60
5	1	6	5	0	50	68	68.33	7.5	9.10
6	1	6	5	4	50	80	79.67	5.44	3.28
7	1	6	25	0	50	83	82.33	6.8	7.62
8	1	6	25	4	50	90	90.67	7.0	11.82
9	1	6	5	2	30	61	61.96	5.05	2.23
10	1	6	5	2	70	84	83.29	5.7	4.94
11	1	6	25	2	30	76	77.46	6.77	6.88
12	1	6	25	2	70	94	92.79	5.28	2.84
13	1	2	15	0	50	75	74.79	5.77	6.40
14	1	10	15	0	50	67	68.63	3.6	1.22
15	1	2	15	4	50	89	90.13	3.4	0.78
16	1	10	15	4	50	71	72.96	3.88	1.5
17	1	6	15	0	30	57	59.04	6.18	6.24
18	1	6	15	0	70	74	76.88	5.4	2.33
19	1	6	15	4	30	67	68.38	5.3	4.01
20	1	6	15	4	70	85	87.21	6.6	3.89
21	1	2	5	2	50	80	83.21	3.45	0.85
22	1	10	5	2	50	69	69.54	5.20	5.61
23	1	2	25	2	50	94	93.71	5.5	4.90
24	1	10	25	2	50	83	84.04	3.65	1.33
25	1	6	15	2	50	81	82.00	5.0	4.14
26	1	6	15	2	50	80	82.00	7.0	7.22
27	1	6	15	2	50	83	82.00	5.3	3.88

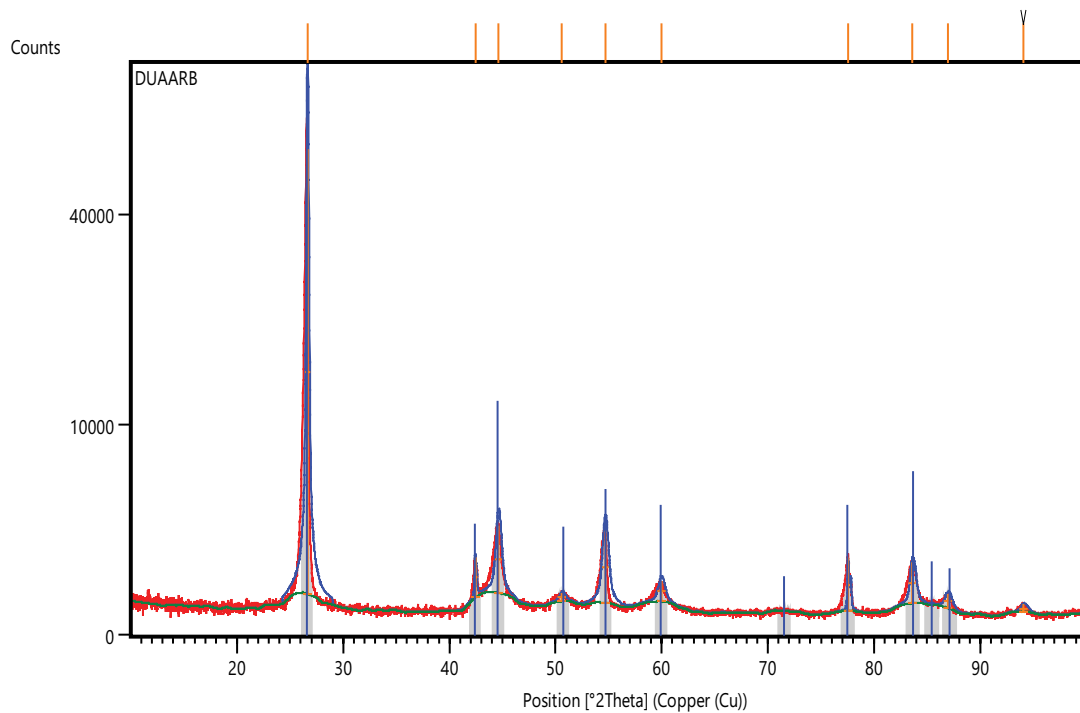


Fig. 2. Graphite's X-ray diffraction pattern.

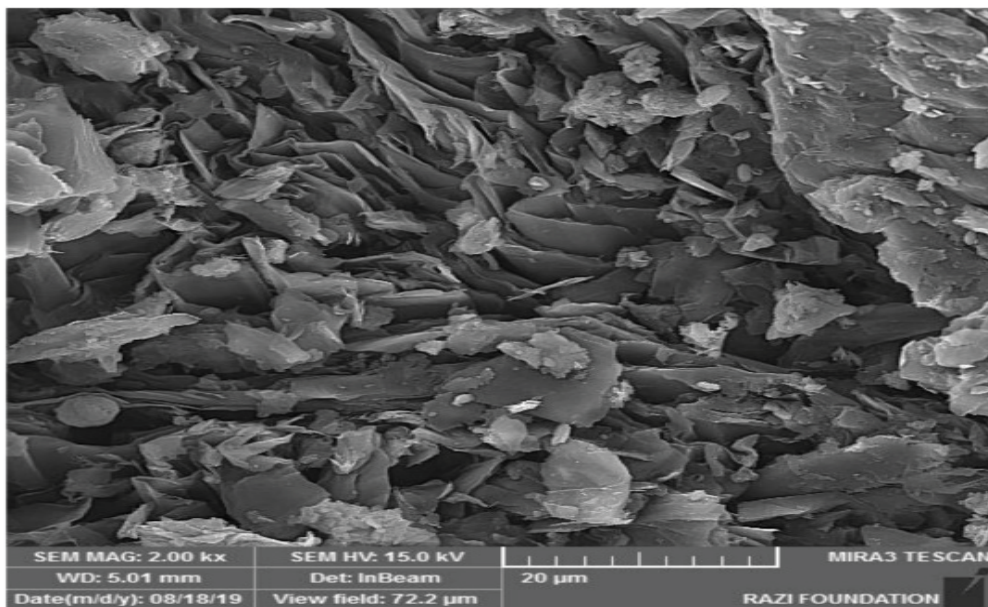


Fig. 3. Porous graphite's scanning electron microscopy picture.

that is greater than the BET of the commercially available graphite felt (SGL carbon, GFA-6 EA) (2.730 m²/g) [43].

3.2. Statistical analyses

A total of 27 statistically designed batch runs for numerous process parameter combinations were done for the optimization and evaluation of collected impacts of

independent factors on efficiency of the removal of COD. Table 3 summarizes experimental findings, which include the percentage of the COD removal (RE%) and specific EC during a 70-min electrolysis time.

The removal efficiency of COD is between 57% and 94%. The energy consumption between 0.62 and 11.82 kWh/kg·COD. The findings of COD removal percentage were analyzed with the use of the Minitab_17 software, and an

experimental link between process parameters and COD removal efficiency was discovered and defined using the quadratic model of the efficiency of the COD removal (RE) in terms of the coded process parameter units:

$$\begin{aligned} \text{Re}\% = & 12.39 + 1.742X_1 - 0.490X_2 + 9.46X_3 + 0.350X_4 \\ & - 0.01260X_1^2 - 0.0807X_2^2 - 1.135X_3^2 + 0.02458X_4^2 \\ & + 0.01250X_1X_2 + 0.0062X_1X_3 - 0.00625X_1X_4 \\ & - 0.3125X_2X_3 + 0.0000X_2X_4 - 0.0625X_3X_4 \end{aligned} \quad (13)$$

where RE% represents response, in other words, percentage of COD removal, and X_1 , X_2 , X_3 and X_4 represent time, pH, concentration of the NaCl, and the current density, respectively. While X_1X_2 , X_1X_3 , X_1X_4 , X_2X_3 , X_2X_4 , X_3X_4 variables represent effect of the interaction of all model parameters. X_1^2 , X_2^2 , X_3^2 and X_4^2 represent measurements of main effects of the variables time, pH, concentration of the NaCl, and the current density, respectively.

Individual variables (linear as well as quadratic) or double interactions impact removal efficiency of COD, as revealed in Eq. (5). Positive coefficient values indicated that there is an increase in removal efficiency of COD when the associated factors regarding such coefficients increased within the established range, whereas negative coefficient values indicated the opposite effect. NaCl concentration, current density, and time all have positive effects on removal efficiency of COD, whereas pH has a negative effect. Table 3 also includes predicted values of the percentage of COD removal that have been calculated with the use of Eq. (5). ANOVA was used for the determination of acceptability of BBD. ANOVA divides total variation in the dataset to individual parts that are accompanied by certain variation sources for examining hypotheses on model factors [44]. The P -test and Fisher F -test are used for determining the model's appropriateness in ANOVA analysis. In the case when Fisher's value is high, the regression equation can clarify the majority of the variations in response. P -value has been utilized for determining whether F is sufficiently great for recognizing statistical significance in the model. When the P -value is $< (0.05)$, 90% of model's variability can be explained [45]. ANOVA for model of response surface is shown in Table 4. The summation of square (Seq. SS), degree of freedom (DF), percentage of contribution (Cr. %), F -value, and P -value for each parameter have been calculated in this table. The regression model had a P -value of 0.0001 and F -value of 74.64, indicating high significance. Model's multiple correlation coefficient has been 98.86%, indicating that regression has statistical significance and that the model only confirms 1.14% of the total variations. In this model, the adjusted multiple correlation coefficient (adj. $R^2 = 97.54\%$) has been in agreement with projected multiple correlation coefficient (predicted $R^2 = 94.07\%$).

The percent contribution regarding the NaCl concentration equals 10.43% that is lower when compared to the other parameters, according to ANOVA results. The current density and pH have roughly the same important impact on process, contributing 18.87% and 15.2%, respectively. With a 40.31% contribution, time has the greatest impact. In the current study, it is clear that both NaCl and pH concentration play a major role in COD removal, implying

that system is regulated via reaction conditions in solution bulk rather than electrooxidation of the ions of the chloride on electrode surface, in other words, the system is under the control of the bulk reaction (chlorine's reaction with water). Linear term contributes the most to this model, accounting for 84.82%, succeeded by square term, which contributes 12.49%, and the 2-way interaction, which contributes 1.55%.

3.3. Effects of the process variables upon efficiency of COD removal

A graphical representation regarding the statistical optimization with the use of RSM was used to analyze the interactive effects of selected parameters and their effect on response. Fig. 4a and b illustrate the effect of initial pH upon percentage of COD removal for varied current densities 5–25 mA/cm² and time 50 min at constant NaCl concentration 2 g/L. The plot of the response surface has been depicted in Fig. 4b, whereas the contour plot is presented in Fig. 4a. The surface plot clearly demonstrates that as the initial pH increases from 2 to 10, COD removal efficiency drops rapidly at current density 5 mA/cm². Scialdone et al. [46] has found that pH has an impact on the efficiency of removal. This way of behaving could be described by the fact that at high values of the pH, active chlorine exist as hypochlorite, that is weaker oxidant toward the organic species when compared to the hypochlorous-acid, which

Table 4
Variance analysis for the removal of chemical oxygen demand

Source	DOF	Seq. SS	Cr. (%)	F -value	P -value
Model	14	2,565.02	98.86	74.64	0.0001
Linear	4	2,278.67	84.82	224.13	0.0001
(X_1)	1	1,083	40.31	426.1	0.0001
(X_2)	1	408.33	15.2	160.66	0.0001
(X_3)	1	280.33	10.43	110.30	0.0001
(X_4)	1	507	18.87	199.48	0.0001
Square	4	335.6	12.49	33.01	0.0001
X_1X_1	1	127.27	4.73	53.34	0.0001
X_2X_2	1	3.8	0.14	3.5	0.086
X_3X_3	1	172.45	6.42	43.28	0.0001
X_4X_4	1	32.23	1.20	12.68	0.004
2-Way Inter.	6	41.75	1.55	2.74	0.065
X_1X_2	1	4	0.15	1.57	0.234
X_1X_3	1	0.25	0.01	0.10	0.759
X_1X_4	1	6.25	0.23	2.46	0.143
X_2X_3	1	25	0.93	9.84	0.009
X_2X_4	1	0	0.0	0.0	1.000
X_3X_4	1	6.25	0.23	2.46	0.143
Error	12	30.5	1.14		
Lack-of-fit	10	25.83	0.96	1.11	0.564
Pure error	2	4.67	0.17		
Total	26	2,686.25	100		
Model summary	5	R^2	R^2 (adj.)	PRESS	R^2 (pred.)
	1.59	98.86%	97.54%	159.3	94.07%

is a powerful oxidant and dominant species at pH levels that are near the value of 2 [46]. The outcomes indicated that the rise of the value of current density from 5 toward 15 mA/cm² had dramatically boosted the efficiency of COD removal at pH 2. In the case when the pH is 10, the same thing happens. The influence of the current density upon COD removal is the same as prior research. This might be indicated by greater formation of hypochlorite in alkaline solution and the hypochlorous acid in acidic solution as current density rises, promoting organic compound breakdown by indirect oxidation [40]. Subsequent contour plot reveals that efficiency of COD removal of 90% is

found in limited area where current density was between 20 and 25 mA/cm² and the pH was in a range between 2 and 5.8.

Fig. 5a shows the influence of the concentration of the NaCl (adding NaCl) on the percentage of the COD removal for various current densities 5–25 mA/cm² at time 50 min and constant pH of 6. At a current density of 5 mA/cm², response surface Fig. 5b reveals that the percentage of the COD removal increases in a linear manner with the rise in NaCl content. At a value of the current density of 25 mA/cm², a comparable pattern emerges. Those findings are consistent with those seen in literature [42]. The matching

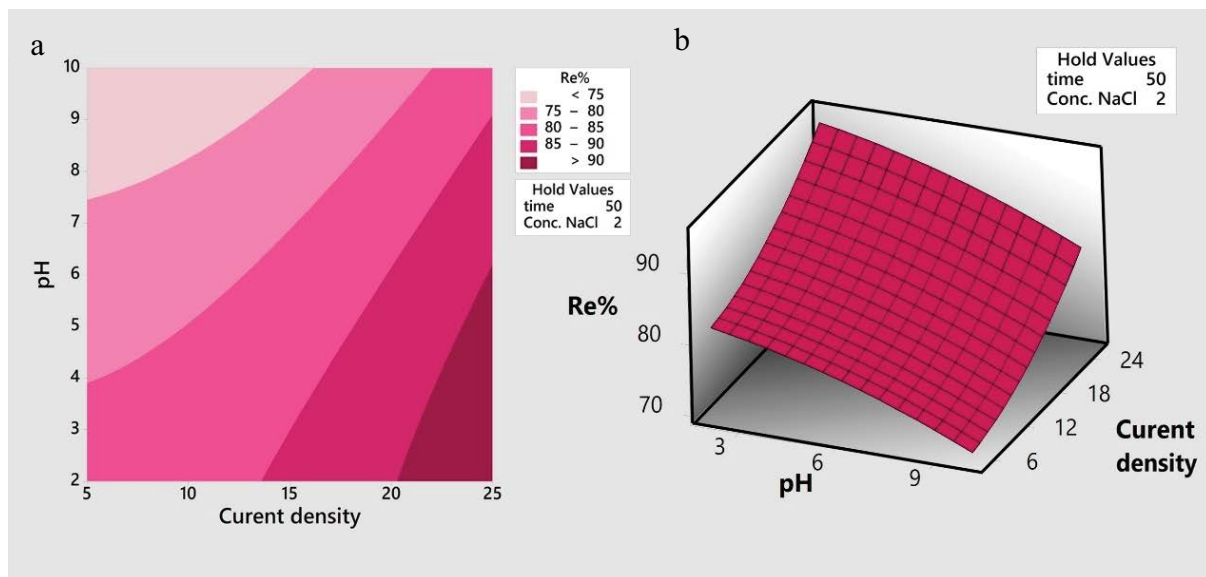


Fig. 4. Contour plot (a) and response surface plot (b) for pH and current density impact upon chemical oxygen demand removal efficiency (RE%) (hold values: NaCl = 2 g/L and time = 50 min).

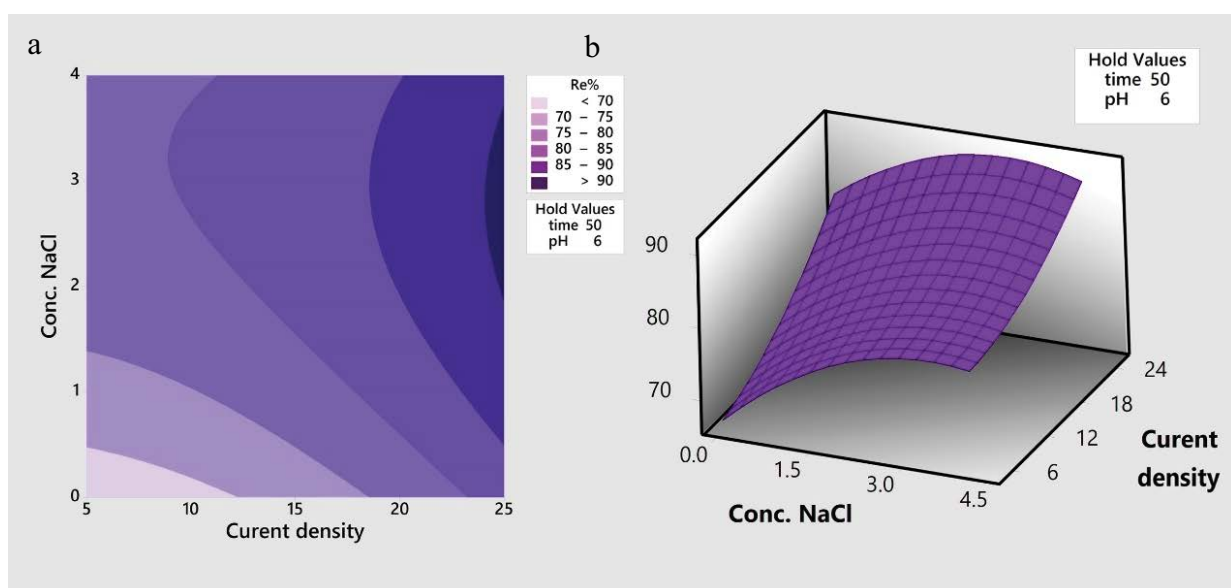


Fig. 5. Contour plot (a) and response surface plot (b) that shows effects of the current density and concentration of NaCl upon efficiency of chemical oxygen demand removal (RE%) (hold values: time = 50min and pH = 6).

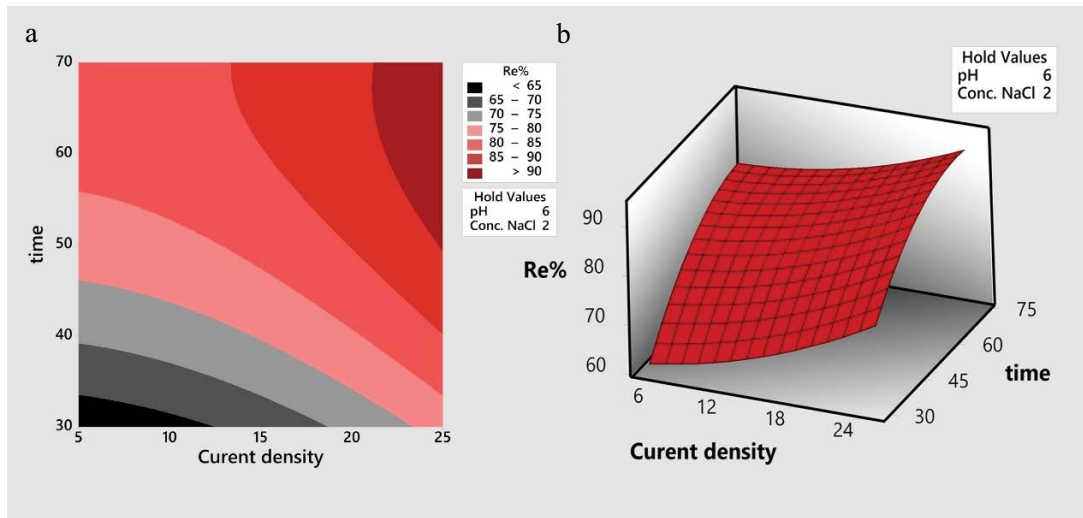


Fig. 6. Contour plot (a) and response surface plot (b) that shows effects of the current density and time upon efficiency of chemical oxygen demand removal (RE%) (hold values: pH = 6 and NaCl = 2 g/L).



Fig. 7. Interaction plot for the efficiency of chemical oxygen demand removal (RE%).

Table 5
Optimal values of the process parameters for the best chemical oxygen demand removal efficiency (RE%)

Responses	Goals	Lower	Target	Upper	Weight	Importance		
RE (%)	Maximal	57	Maximum	94	1	1		
Solution: parameters				Results				
Current density (mA/cm ²)	pH	NaCl (g/L)	Time (min)	RE (%) Fit	DF	SE Fit	95%CI	95%PI
25	2	3.39	64.74	99.6	1	1.82	(95.64; 103.56)	(94.34; 104.86)

Table 6
Confirmative value regarding optimal removal efficiency of chemical oxygen demand

Run	Current density (mA/cm ²)	pH	NaCl (g/L)	Time (min)	E (Volt)	Chemical oxygen demand (ppm)		RE (%)		EC (kWh/kg-COD)
						Initial	Final	Actual	Average	
1	25	2	3.4	65	6.1	572	7	99.55	99.1	9.95
2	25	2	3.4	65	6.0	569	2	98.77		
3	25	10	3.4	65	5.9	585	23	91.65		9.68

contour Fig. 5a reveals that the removal efficiency of $\geq 90\%$ is found in a limited area where the current density was 23–25 mA/cm² and NaCl was added at a concentration of 2–3.8 g/L. Fig. 6a and b illustrate influence of time on COD removal percentage for different current densities 5–25 mA/cm² at constant NaCl concentration 2 g/L and pH value of 6. Fig. 6b demonstrates how, at low current density, COD removal increases rapidly with the rise of time. When the current density reached 25 mA/cm², the same behavior was detected. Those findings are consistent with those seen in literature [39,40,42]. The related contour Fig. 6a reveals that the efficiency of removal of 90% is found in limited area with current densities ranging between 21 to 25 mA/cm² and times ranging between 50 to 70 min. As a result, using RSM will help to determine the achievable optimal values of the elements being investigated, as well as providing useful facts on the interactions between them. Fig. 7 depicts the COD removal efficiency interaction plot among process parameters. There was no significant interaction between factors, as can be observed.

3.3. Optimization and confirmation test

The optimization regarding any electrochemical removal system's process conditions is vital and must be accomplished for the purpose of minimizing energy losses and, as a result, treatment cost losses. Various principles were found for improving the system in order to achieve the intended goal by maximizing the desirability function (DF) by adapting the importance or weight that might alert the properties of the objective. There are five options for the target fields for variables: maximize, none, objective, minimize, and within range. The 'maximum' with the associated 'weight' 1.0 is the target of electrochemical COD removal. The independent factors that were investigated in this research have been set within the range of specified levels (pH: 2–10, current: 5–25 mA/cm², time: 30–70 min, and NaCl: 0–4 g/L).

The COD removal efficiency lower limit has been set at 57%, whereas upper limit has been set at 94%. Table 5 shows outcomes of the optimization technique using such settings and boundaries, with the function of desirability of 1. Two confirmative tests have been carried out utilizing optimized parameters for their validation, results of which have been shown from Table 6. A 94% efficiency of COD removal was attained as a mean value following 70 min of electrolysis at pH = 2, which is within the range of the optimal values that have been obtained via optimization analysis using the function of desirability of 1 (Table 6). As a result, using the Box–Behnken design in conjunction with the desirability function to optimize COD removal with the use of porous graphite anode is effective. Additional set of experiments was carried out under similar optimum parameters, with the exception that the initial pH was set to 10 rather than 2. The results demonstrate that COD removal effectiveness was 91.5% in this example, resulting in a final COD level of 43 ppm, which is lower than permitted limit that has been set by Al-Najaf petroleum refinery plant management (Table 1).

4. Conclusions

The goal of this study is to see how different operating parameters like initial pH, current density, time, and NaCl concentration affected the COD removal in treatment of Al-Najaf petroleum refinery wastewater with the use of an indirect process of the anodic oxidation on porous graphite anode and BBD as optimization approach. Experimental data was used to fit second-order polynomial equation that has been then used for the regulation of the operating parameters. The optimal circumstances were NaCl concentration of 3.4 g/L, current density of 25 A/cm², an electrolysis time of 64 min, a pH of 2, which resulted in a 99.6% COD removal efficiency and a 9.85 kWh/kg energy consumption of COD. The results demonstrate that in the current study, both NaCl and pH concentration have a major impact on

COD removal, implying that the system is regulated through conditions of reaction in bulk of the solution rather than electro-oxidation reaction on electrode surface. The majority of mechanisms regarding indirect anodic oxidation reaction published in literature had agreed with this.

Acknowledgement

The authors acknowledge the supportive and practical assistance provided by the staff of Chemical Engineering and petroleum industries Dept., Al-Mustaqbal University College.

References

- [1] M.N. Rahi, A.J. Jaeel, A.J. Abbas, Treatment of petroleum refinery effluents and wastewater in Iraq: a mini review, *IOP Conf. Ser.: Mater. Sci. Eng.*, 1058 (2021) 012072, doi: 10.1088/1757-899X/1058/1/012072.
- [2] D.A. Aljuboury, P. Palaniandy, H.B. Abdul Aziz, S. Feroz, Treatment of petroleum wastewater by conventional and new technologies - a review, *Global Nest J.*, 19 (2017) 439–452.
- [3] T.E. Welch, *Moving Beyond Environmental Compliance: A Handbook for Integrating Pollution Prevention with ISO 14000*, CRC Press, Boca Raton, 2018.
- [4] I. Phummiphan, S. Horpibulsuk, R. Rachan, A. Arulrajah, S.-L. Shen, P. Chindaprasirt, Corrigendum to "high calcium fly ash geopolymer stabilized lateritic soil and granulated blast furnace slag blends as a pavement base material, *J. Hazard. Mater.*, 341 (2018) 257–267.
- [5] F. Shahrezaei, Y. Mansouri, A.A.L. Zinatizadeh, A. Akhbari, Process modeling and kinetic evaluation of petroleum refinery wastewater treatment in a photocatalytic reactor using TiO₂ nanoparticles, *Powder Technol.*, 221 (2012) 203–212.
- [6] M.R. Esfahani, S.A. Aktij, Z. Dabaghian, M.D. Firouzjaei, A. Rahimpour, J. Eke, I.C. Escobar, M. Abolhassani, L.F. Greenlee, A.R. Esfahani, Nanocomposite membranes for water separation and purification: fabrication, modification, and applications, *Sep. Purif. Technol.*, 213 (2019) 465–499.
- [7] S.M. Jiménez, M.M. Micó, M. Arnaldos, F. Medina, S. Contreras, State-of-the-art of produced water treatment, *Chemosphere*, 192 (2018) 186–208.
- [8] K. Zuo, M. Chen, F. Liu, K. Xiao, J. Zuo, X. Cao, X. Zhang, P. Liang, X. Huang, Coupling microfiltration membrane with biocathode microbial desalination cell enhances advanced purification and long-term stability for treatment of domestic wastewater, *J. Membr. Sci.*, 547 (2018) 34–42.
- [9] C.E. Santo, V.J.P. Vilar, C.M.S. Botelho, A. Bhatnagar, E. Kumar, R.A.R. Boaventura, Optimization of coagulation–flocculation and flotation parameters for the treatment of a petroleum refinery effluent from a Portuguese plant, *Chem. Eng. J.*, 183 (2012) 117–123.
- [10] E. Güneş, E. Demir, Y. Güneş, A. Hanedar, Characterization and treatment alternatives of industrial container and drum cleaning wastewater: comparison of Fenton-like process and combined coagulation/oxidation processes, *Sep. Purif. Technol.*, 209 (2019) 426–433.
- [11] S. Martini, S. Afroz, K.A. Roni, Modified eucalyptus bark as a sorbent for simultaneous removal of COD, oil, and Cr(III) from industrial wastewater, *Alexandria Eng. J.*, 59 (2020) 1637–1648.
- [12] M.A. Hussein, A.A. Mohammed, M.A. Atiya, Application of emulsion and Pickering emulsion liquid membrane technique for wastewater treatment: an overview, *Environ. Sci. Pollut. Res.*, 26 (2019) 36184–36204.
- [13] A.A. Mohammed, M.A. Atiya, M.A. Hussein, Studies on membrane stability and extraction of ciprofloxacin from aqueous solution using Pickering emulsion liquid membrane stabilized by magnetic nano-Fe₃O₄, *Colloids Surf., A*, 585 (2020) 124044, doi: 10.1016/j.colsurfa.2019.124044.
- [14] S. Munirasu, M.A. Haija, F. Banat, Use of membrane technology for oil field and refinery produced water treatment—a review, *Process Saf. Environ. Prot.*, 100 (2016) 183–202.
- [15] J. Ma, R. Dai, M. Chen, S.J. Khan, Z. Wang, Applications of membrane bioreactors for water reclamation: micropollutant removal, mechanisms and perspectives, *Bioresour. Technol.*, 269 (2018) 532–543.
- [16] L. Altaş, H. Büyükgüngör, Sulfide removal in petroleum refinery wastewater by chemical precipitation, *J. Hazard. Mater.*, 153 (2008) 462–469.
- [17] T.-K. Tran, K.-F. Chiu, C.-Y. Lin, H.-J. Leu, Electrochemical treatment of wastewater: selectivity of the heavy metals removal process, *Int. J. Hydrogen Energy*, 42 (2017) 27741–27748.
- [18] X. Niu, X. Li, J. Pan, Y. He, F. Qiu, Y. Yan, Recent advances in non-enzymatic electrochemical glucose sensors based on non-precious transition metal materials: opportunities and challenges, *RSC Adv.*, 6 (2016) 84893–84905.
- [19] M. Panizza, G. Cerisola, Direct and mediated anodic oxidation of organic pollutants, *Chem. Rev.*, 109 (2009) 6541–6569.
- [20] S. Rajoriya, S. Bargole, S. George, V.K. Saharan, Treatment of textile dyeing industry effluent using hydrodynamic cavitation in combination with advanced oxidation reagents, *J. Hazard. Mater.*, 344 (2018) 1109–1115.
- [21] S. Singh, S.L. Lo, V.C. Srivastava, A.D. Hiwarkar, Comparative study of electrochemical oxidation for dye degradation: parametric optimization and mechanism identification, *J. Environ. Chem. Eng.*, 4 (2016) 2911–2921.
- [22] I.D. Santos, J.C. Afonso, A.J.B. Dutra, Behavior of a Ti/RuO₂ anode in concentrated chloride medium for phenol and their chlorinated intermediates electrooxidation, *Sep. Purif. Technol.*, 76 (2010) 151–157.
- [23] C.A. Martínez-Huitle, L.S. Andrade, Electrocatalysis in wastewater treatment: recent mechanism advances, *Quim. Nova*, 34 (2011) 850–858.
- [24] S. Abbasi, M. Mirghorayshi, S. Zinadini, A.A. Zinatizadeh, A novel single continuous electrocoagulation process for treatment of licorice processing wastewater: optimization of operating factors using RSM, *Process Saf. Environ. Prot.*, 134 (2020) 323–332.
- [25] K.K. Salam, A.O. Arinkoola, E.O. Oke, J.O. Adeleye, Optimization of operating parameters using response surface methodology for paraffin-wax deposition in pipeline, *Pet. Coal*, 56 (2014) 19–28.
- [26] A.R. Matin, S. Yousefzadeh, E. Ahmadi, A. Mahvi, M. Alimohammadi, H. Aslani, R. Nabizadeh, A comparative study of the disinfection efficacy of H₂O₂/ferrate and UV/H₂O₂/ferrate processes on inactivation of *Bacillus subtilis* spores by response surface methodology for modeling and optimization, *Food Chem. Toxicol.*, 116 (2018) 129–137.
- [27] K. Hendaoui, F. Ayari, I.B. Rayana, R.B. Amar, F. Darragi, M. Trabelsi-Ayadi, Real indigo dyeing effluent decontamination using continuous electrocoagulation cell: study and optimization using response surface methodology, *Process Saf. Environ. Prot.*, 116 (2018) 578–589.
- [28] H. Zhang, Y. Li, X. Zhong, X. Ran, Application of experimental design methodology to the decolorization of Orange II using low iron concentration of photoelectro-Fenton process, *Water Sci. Technol.*, 63 (2011) 1373–1380.
- [29] M. Darvishmotevalli, A. Zarei, M. Moradnia, M. Noorisepehr, H. Mohammadi, Optimization of saline wastewater treatment using electrochemical oxidation process: prediction by RSM method, *MethodsX*, 6 (2019) 1101–1113.
- [30] J. de Jesús Treviño-Reséndez, A. Medel, Y. Meas, Electrochemical technologies for treating petroleum industry wastewater, *Curr. Opin. Electrochem.*, 27 (2021) 100690, doi: 10.1016/j.coelec.2021.100690.
- [31] L.C. Espinoza, C. Candia-Onfray, J. Vidal, R. Salazar, Influence of the chemical nature of boron-doped diamond anodes on wastewater treatments, *Curr. Opin. Solid State Mater. Sci.*, 25 (2021) 100963, doi: 10.1016/j.cossms.2021.100963.
- [32] C.A. Martínez-Huitle, E. Brillas, A critical review over the electrochemical disinfection of bacteria in synthetic and real

- wastewaters using a boron-doped diamond anode, *Curr. Opin. Solid State Mater. Sci.*, 25 (2021) 100926, doi: 10.1016/j.cossms.2021.100926.
- [33] H. Ajab, M.H. Isa, A. Yaqub, Electrochemical oxidation using Ti/RuO₂ anode for COD and PAHs removal from aqueous solution, *Sustainable Mater. Technol.*, 26 (2020) e00225, doi: 10.1016/j.susmat.2020.e00225.
- [34] A.N. Ghanim, A.S. Hamza, Evaluation of direct anodic oxidation process for the treatment of petroleum refinery wastewater, *J. Environ. Eng.*, 144 (2018) 04018047, doi: 10.1061/(ASCE)EE.1943-7870.0001389.
- [35] J. Ma, M. Gao, H. Shi, J. Ni, Y. Xu, Q. Wang, Progress in research and development of particle electrodes for three-dimensional electrochemical treatment of wastewater: a review, *Environ. Sci. Pollut. Res.*, 28 (2021) 47800–47824.
- [36] W. Li, G. Liu, D. Miao, Z. Li, Y. Chen, X. Gao, T. Liu, Q. Wei, L. Ma, K. Zhou, Electrochemical oxidation of Reactive Blue 19 on boron-doped diamond anode with different supporting electrolyte, *J. Environ. Chem. Eng.*, 8 (2020) 103997, doi: 10.1016/j.jece.2020.103997.
- [37] O. Abdelwahab, N.K. Amin, E.Z. El-Ashtoukhy, Electrochemical removal of phenol from oil refinery wastewater, *J. Hazard. Mater.*, 163 (2009) 711–716.
- [38] S. Sharma, H. Simsek, Treatment of canola-oil refinery effluent using electrochemical methods: a comparison between combined electrocoagulation + electrooxidation and electrochemical peroxidation methods, *Chemosphere*, 221 (2019) 630–639.
- [39] H.A. Shamkhi, A.D.Z. Albdiri, F.A. Jabir, D. Petruzzelli, Removal of Pb²⁺, Cu²⁺, and Cd²⁺ ions from a saline wastewater using emulsion liquid membrane: applying response surface methodology for optimization and data analysis, *Arabian J. Sci. Eng.*, 47 (2022) 5705–5719.
- [40] N. Sadati, R.B. Chinnam, M.Z. Nezhad, Observational data-driven modeling and optimization of manufacturing processes, *Expert Syst. Appl.*, 93 (2018) 456–464.
- [41] Y.-D. Chen, W.-Q. Chen, B. Huang, M.-J. Huang, Process optimization of K₂C₂O₄-activated carbon from kenaf core using Box–Behnken design, *Chem. Eng. Res. Des.*, 91 (2013) 1783–1789.
- [42] A.N. Popova, Crystallographic analysis of graphite by X-ray diffraction, *Coke Chem.*, 60 (2017) 361–365.
- [43] H.R. Jiang, W. Shyy, M.C. Wu, R.H. Zhang, T.S. Zhao, A bi-porous graphite felt electrode with enhanced surface area and catalytic activity for vanadium redox flow batteries, *Appl. Energy*, 233 (2019) 105–113.
- [44] I. Saravanan, A.E. Perumal, S.C. Vettivel, N. Selvakumar, A. Baradeswaran, Optimizing wear behavior of TiN coated SS 316L against Ti alloy using response surface methodology, *Mater. Des.*, 67 (2015) 469–482.
- [45] M. Xu, D. Jin, E. Song, Parameter Identification of the High-Fill Foundations Using Response Surface Method, W. Wu, H.S. Yu, Eds., *Proceedings of China-Europe Conference on Geotechnical Engineering*, Springer Series in Geomechanics and Geoengineering, Springer, Cham, 2018, pp. 1055–1058. https://doi.org/10.1007/978-3-319-97115-5_37
- [46] O. Scialdone, S. Randazzo, A. Galia, G. Silvestri, Electrochemical oxidation of organics in water: role of operative parameters in the absence and in the presence of NaCl, *Water Res.*, 43 (2009) 2260–2272.